Engineering 51 (2025) 37–48

Contents lists available at ScienceDirect

Engineering

journal homepage: www.elsevier.com/locate/eng

Research
Smart Grid and Energy Internet—Article

Optimal Peer-to-Peer Coupled Electricity and Carbon Trading in Distribution Networks

Huangqi Ma [a], Yue Xiang [a,*], Alexis Pengfei Zhao [b], Shuangqi Li [c], Junyong Liu [a]

[a] College of Electrical Engineering, Sichuan University, Chengdu 610065, China
[b] Department of Energy Science and Engineering, Stanford Doerr School of Sustainability, Stanford University, Stanford, CA 94305, USA
[c] Department of Electrical and Electronic Engineering, Research Centre for Grid Modernization, The Hong Kong Polytechnic University, Hong Kong 999077, China

ARTICLE INFO

Article history:
Received 26 June 2024
Revised 6 January 2025
Accepted 19 January 2025
Available online 23 January 2025

Keywords:
Prosumer
Network charge
Carbon-emission rights
Peer-to-peer trading

ABSTRACT

The surge of distributed renewable energy resources has given rise to the emergence of prosumers, facilitating the low-carbon transition of distribution networks. However, flexible prosumers introduce bidirectional power and carbon interaction, increasing the complexity of practical decision-making in distribution networks. To address these challenges, this paper presents a carbon-coupled network charge-guided bi-level interactive optimization method between the distribution system operator and prosumers. In the upper level, a carbon-emission responsibility settlement method that incorporates the impact of peer-to-peer (P2P) trading is proposed, based on a carbon-emission flow model and optimal power flow model, leading to the formulation of carbon-coupled network charges. In the lower level, a decentralized P2P trading mechanism is developed to achieve the clearing of energy and carbon-emission rights. Furthermore, an alternating direction method of multipliers with an adaptive penalty factor is introduced to address the equilibrium of the P2P electricity–carbon coupled market, and an improved bisection method is employed to ensure the convergence of the bi-level interaction. A case study on the modified IEEE 33-bus system demonstrates the effectiveness of the proposed model and methodology.

1. Introduction

The profound threat posed by global warming to natural ecosystems and human development has garnered widespread attention [1]. Addressing climate change, reducing carbon emissions, and implementing sustainable development strategies have become shared goals among nations around the world. The consumption of fossil fuels by thermal power plants is a significant global source of carbon emissions [2]. Prosumers, which are capable of generating electricity from distributed renewable energy sources (RES), are rapidly increasing in number due to their ability to promote energy emission reduction. In this context, prosumers can achieve energy trading and sharing through peer-to-peer (P2P) trading, which are one method to enhance the utilization rate of distributed renewable energy and meet carbon-reduction targets [3]. However, prosumers must bear the costs associated with carbon reduction while considering carbon-reduction targets. Therefore, it is crucial for prosumers to effectively coordinate their electricity demand with their carbon emissions, which is essential for achieving sustainable economic development.

The electricity–carbon coupled trading market is viewed as a viable solution to the aforementioned challenges. Within this market, prosumers can purchase the required energy and carbon-emissions rights (CER) through both the electricity market and the CER market. P2P trading, as an emerging energy trading model, can effectively facilitate decentralized, flexible, and autonomous trading [4]. The P2P trading mechanism has been recognized as an effective approach to prosumer electricity trading [5]. In the CER trading market, market participants can sell or buy corresponding CER to ensure their emissions are within carbon-emission allowances. The price of CER in this market is determined by market competition, similar to the energy trading market [6]. Thus, in a market environment where electricity and CER are coupled, the P2P mechanism can serve as an effective coordination framework [7].

Current P2P solutions include bilateral contract-based methods [8], game-theoretic-based methods [9,10], auction schemes

* Corresponding author.
E-mail address: xiang@scu.edu.cn (Y. Xiang).

https://doi.org/10.1016/j.eng.2025.01.006

[11,12], and distributed algorithmic approaches [13,14]. The bilateral contract-based method, as presented in Ref. [8], introduces bilateral contract networks as a new scalable market design for P2P energy trading to mitigate the impact of uncertainty. Game-theoretic-based methods consider the mutual influence of prosumer decision-making and describe the competition among prosumers using game theory. Ref. [9] established a P2P energy-sharing scenario based on the Stackelberg leader–follower game that minimizes carbon and energy costs while enhancing prosumer benefit. Ref. [10] formulated the P2P coupled market as a risk-averse stochastic Stackelberg game and proved its Stackelberg equilibrium. Unlike game theory models, the bilateral auction process involves a centralized clearing process to achieve energy clearing. Ref. [11] proposed a combinatorial auction method to address resource allocation among prosumers in residential communities, and Ref. [12] employed a multi-round double auction method to facilitate the energy-clearing process for multiple prosumers. In recent years, numerous studies have focused on trading negotiation schemes between prosumers without the involvement of a distribution system operator (DSO) and have employed decentralized trading negotiation processes facilitated by distributed algorithms, such as the subgradient method [13] and the multiplier alternating direction method [14].

Achieving P2P electricity–carbon coupled trading among prosumers still presents two primary challenges: ① How can electricity–carbon market coupled trading be implemented, and how can the carbon emissions of prosumers be accurately calculated; and ② as P2P energy trading requires physical network delivery from the actual power distribution network, how can prosumers conduct economical low-carbon trading while ensuring network security?

To address the first challenge, the coupling of electricity and carbon markets can be reflected by incorporating the value of transactional CER into energy pricing, thereby influencing prosumer trading preferences and ultimately achieving cost-effective decarbonization [15]. The introduction of the bilateral carbon trading concept provides a new approach for the allocation of carbon-emission responsibilities [16], by tracing carbon emissions and allocating responsibilities to both generators and consumers. Ref. [17] proposed a bi-level multi-energy system planning model with the interaction of two markets, using the carbon-emission flow (CEF) model to calculate emissions from the demand side with regional emission constraints. Ref. [18] presented a two-stage scheduling model applying the CEF model to track carbon flows, demonstrating the feasibility of carbon-oriented operational planning. Ref. [19] established a CEF model for an integrated electricity–gas–heat energy system, quantifying CEFs coupled with multiple types of energy flows. Ref. [20] introduced an integrated energy–carbon pricing method for multi-energy systems. However, due to the intricate structure of the distribution network and the scarcity of downstream carbon-emission monitoring points, it was not feasible to track individual user carbon-emission intensities. As a result, the carbon pricing was determined based on the weighted carbon intensity of various nodes, thereby incorporating carbon-emission costs into the transmission and distribution side. However, the different trading behaviors of prosumers in local energy trading lead to different CEFs, and further research is required on how to allocate carbon-emission responsibilities based on the distinct trading behaviors of prosumers.

For the second challenge, network charges are considered an effective way to incentivize prosumers by transferring the responsibility of network security constraints to them, thereby turning the reduction of system risks into a self-motivated goal for prosumers [21]. Existing network charge strategies mainly include electrical distance costs [22], regional cost-allocation strategies [23], and distribution locational marginal price (DLMP) [24]. The authors of Ref. [22] calculated the transmission fee using the electrical distance method and incorporated it into the prosumer trading negotiation decision phase. Ref. [23] used the regional cost-allocation method for network usage cost sharing, influencing P2P trading decisions. Ref. [24], based on the second-order conic alternating current (AC)-optimal power flow (OPF) model of the distribution network, used the difference in DLMP to calculate the network usage charges that prosumers should pay, ultimately ensuring the secure operation of the network. In summary, guiding prosumers to voluntarily adjust their trading behaviors through price signals greatly enhances prosumer enthusiasm and economic efficiency. However, the aforementioned network charges, while effectively guiding prosumer trading behaviors, are operationally oriented and do not reflect the carbon intensity in the network, making it difficult to assess the carbon-reduction benefits of each transaction. Therefore, existing network charge strategies lack carbon-oriented costs to guide low-carbon trading, and it is necessary to propose a carbon-coupled network pricing method to guide prosumers in conducting grid-friendly and low-carbon trading that respects network operational constraints.

This paper introduces a bi-level interactive optimization method guided by carbon-coupled network charges between the DSO and prosumers, aiming to accurately steer prosumer trading to achieve safe and low-carbon operation of the distribution network. The main contributions of this paper are as follows:

(1) A bi-level interactive framework is proposed, integrating the economic aspects of energy trading with the operational requirements for low-carbon and secure distribution network management. This framework includes a carbon-emission responsibility settlement method that accounts for the impact of P2P trading, enabling an accurate allocation of carbon responsibilities within the bi-level model.

(2) The introduction of the carbon-coupled network charges captures the influence of P2P coupled trading on network security and emission reduction. These charges reflect the associated carbon costs and network risks, effectively guiding prosumers toward low-carbon trading while adhering to the security constraints of the distribution network.

(3) A decentralized trading priority method for P2P trading is presented, which uses economic incentives at the prosumer level to facilitate the trade of electricity and CER. This method not only aligns with the trading preferences of prosumers but also reduces energy costs for both parties involved. To address the complexity of the P2P coupled market trading model, an alternating direction method of multipliers (ADMM) with an adaptive penalty factor is utilized to expedite the solution process. Furthermore, a limited information-sharing approach is employed between prosumers and the DSO to solve their respective optimization problems, with an iterative calculation process converging toward a stable optimal solution. An improved bisection method is also utilized to ensure the convergence of the DSO–prosumers bi-level interactive problem.

The rest of this paper is organized as follows. The proposed bi-level interactive framework is introduced in Section 2. Section 3 establishes the utility function for prosumers participating in the P2P coupled market. Section 4 develops the DSO optimization model and illustrates the carbon-coupled network charges model. Section 5 presents the solution algorithm for the bi-level model. Section 6 provides a case study. Finally, Section 7 concludes the paper.

2. Market framework

To achieve optimal P2P electricity and carbon trading among prosumers, we have designed a DSO–prosumers bi-level interactive framework. This framework integrates electricity–carbon coupled market trading with the operation of distribution networks,

thereby simultaneously enhancing the benefits of market participants and ensuring the low-carbon and secure operation of the system. In the electricity–carbon coupled P2P trading market, prosumers with RES can engage in energy and CER trading through the electricity and carbon market. Prosumers autonomously determine the quantity of energy and CER to trade, offsetting their own carbon emissions while maximizing their profits. Incorporating the CER market into the energy system can significantly alter prosumers' energy trading and power-generation patterns through carbon pricing that is proportional to their carbon content. In this context, trading among prosumers is conducive to decarbonizing the current energy system.

At the upper level, the DSO operates the network based on prosumer trading results, ensuring network security based on the OPF model and deriving operational network charges from the DLMP. Concurrently, the CEF model is utilized to track carbon emissions post-P2P trading, obtaining the carbon distribution and calculating carbon-coupled network charges. The DSO guides P2P trading between prosumers through price signals rather than direct control, safeguarding prosumers' autonomy and privacy. Additionally, updated network charges will adjust P2P trading scenarios in the subsequent iteration.

In the lower level of the energy and CER trading market, prosumers engage in P2P trading for energy and CER. The DSO can indirectly guide their trading behavior by conveying carbon-coupled network charges information to prosumers, effectively steering low-carbon trading without violating distribution network security constraints. Market-clearing algorithms then complete the clearing of the P2P coupled market, conveying trading outcomes to the DSO for secure distribution network scheduling. The bi-level interactive model is depicted in Fig. 1.

It is important to note that the prosumers' energy trading characteristics are predefined, allowing them to acquire additional power through the electricity market to address energy deficits. However, the carbon trading attribute of a prosumer is determined dynamically by the prosumer's P2P energy trading. This implies that prosumers, who may initially lack CER, can acquire them by purchasing from other prosumers in the market. The bi-level model operates in an iterative, interactive manner, continually adjusting until equilibrium is reached in the P2P market's trading outcomes.

3. The electricity–carbon coupled market

In the coupled market, recognizing the disparities among prosumers, such as geographical location, distribution of flexible resources, and user types, we categorize them into two distinct categories. The first category consists of prosumers who actively embrace low-carbon policy changes, referred to as "novel" prosumers. Conversely, the second category encompasses "traditional" prosumers with substantial carbon emissions from their fossil-fuel-based systems. Prosumers of both types have distinct advantages and disadvantages. To increase their profits, prosumers need to determine the optimal trading strategy within the coupled market that best aligns with their operations.

3.1. Internal model for prosumers

3.1.1. Gas turbines (GTs)

The cost of electricity generation from a GT is typically modeled as a quadratic function [25] and can be mathematically represented as follows:

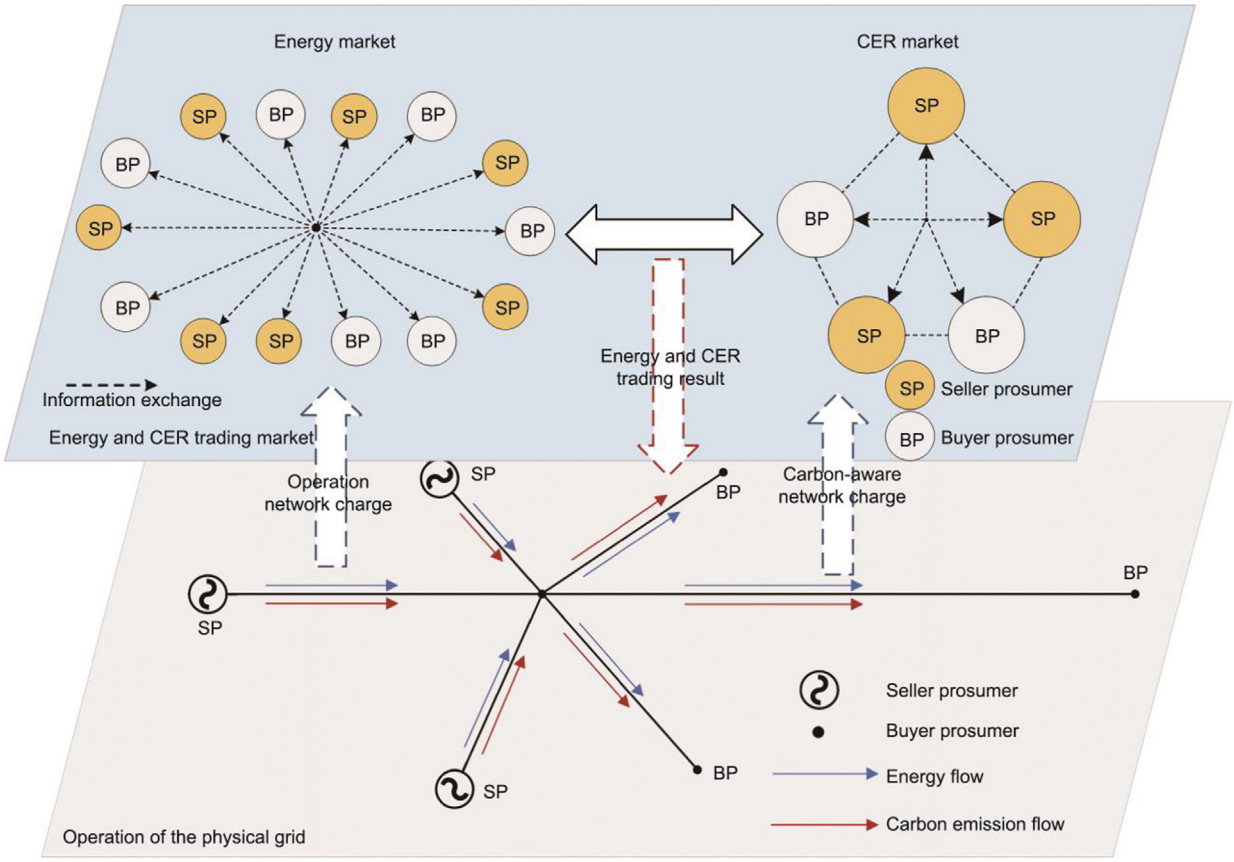

Fig. 1. The bi-level interactive model.

$$C_{n,t}^{\mathrm{G}}=\frac{1}{2}a_n^{\mathrm{G}}\left(P_{n,t}^{\mathrm{G}}\right)^2+b_n^{\mathrm{G}}P_{n,t}^{\mathrm{G}} \tag{1}$$

where $C_{n,t}^{\mathrm{G}}$ is the power-generation cost of the GT; a_n^{G} and b_n^{G} represent the cost factor of the generator set, respectively; $P_{n,t}^{\mathrm{G}}$ is GT output power of prosumer n, and t is the index of operation/trading interval.

3.1.2. Photovoltaics (PV)

PV technology harnesses solar energy through the photoelectric effect of solar panels, converting sunlight into electricity. The power output is directly proportional to the intensity of solar radiation. The power model of PVs is as follows:

$$I_{\mathrm{ac}}=I_{n,\mathrm{STC}}\cdot\frac{F_{n,t}}{F_{n,\mathrm{STC}}}\cdot[1+\alpha(T_{\mathrm{ac}}-T_0)] \tag{2}$$

$$V_{\mathrm{ac}}=V_{n,\mathrm{STC}}\cdot\ln[\mathrm{e}+\beta(F_{n,t}-F_{n,\mathrm{STC}})][1-\zeta(T_{\mathrm{ac}}-T_0)] \tag{3}$$

$$P_{n,t}^{\mathrm{PV}}=N_{\mathrm{m}}\cdot I_{\mathrm{ac}}\cdot V_{\mathrm{ac}} \tag{4}$$

where T_0 and T_{ac} are the reference temperature and the operating temperature of the PV array, respectively; I_{ac} and V_{ac} are the output current and voltage of the PV, respectively; $I_{n,\mathrm{STC}}$ and $V_{n,\mathrm{STC}}$ are the rated output current and voltage of the PV, respectively; $F_{n,t}$ and $F_{n,\mathrm{STC}}$ are the actual solar irradiance and the standard solar irradiance, respectively; N_{m} is the number of PV panels; α, β, and ζ are the compensation factor sets, respectively; and $P_{n,t}^{\mathrm{PV}}$ is PV output power of prosumer n.

3.1.3. Energy storage (ES)

ES can generate profit by making it possible to strategically purchase low-cost electricity and selling it at a higher price. However, excessive charging and discharging can negatively impact a battery's lifespan. Consequently, a cost model for the ES charging and discharging activities is formulated as follows:

$$C_{n,t}^{\mathrm{ES}}=f_n^{\mathrm{ES}}(P_{n,t}^{\mathrm{ES,cha}}+P_{n,t}^{\mathrm{ES,dis}}) \tag{5}$$

The charge–discharge constraints of ES are as follows:

$$0\le P_{n,t}^{\mathrm{ES,cha}}\le\eta_{n,t}^{\mathrm{ES}}P_{n,t}^{\mathrm{ES,cha_{max}}} \tag{6}$$

$$0\le P_{n,t}^{\mathrm{ES,dis}}\le(1-\eta_{n,t}^{\mathrm{ES}})P_{n,t}^{\mathrm{ES,dis_{max}}} \tag{7}$$

$$\mathrm{SOC}_n^{\mathrm{ES,min}}\le\mathrm{SOC}_{n,t}^{\mathrm{ES}}\le\mathrm{SOC}_n^{\mathrm{ES,max}} \tag{8}$$

where $C_{n,t}^{\mathrm{ES}}$ is charging and discharging costs of ES; f_n^{ES} is operation cost coefficient of ES; $P_{n,t}^{\mathrm{ES,cha}}$ and $P_{n,t}^{\mathrm{ES,dis}}$ are ES charge and discharge power of prosumer n, respectively; $\eta_{n,t}^{\mathrm{ES}}$ is ES charging states; $P_{n,t}^{\mathrm{ES,cha_{max}}}$ and $P_{n,t}^{\mathrm{ES,dis_{max}}}$ are maximum amount of charge and discharge for ES, respectively; $\mathrm{SOC}_{n,t}^{\mathrm{ES}}$ is SOC status of ES; and $\mathrm{SOC}_n^{\mathrm{ES,min}}$ and $\mathrm{SOC}_n^{\mathrm{ES,max}}$ are minimum and maximum SOC status of ES, respectively.

3.1.4. Electric vehicles (EVs)

In the rapidly advancing landscape of EVs, a growing number of residential prosumers possess EVs. The operation and scheduling of these EVs have a corresponding impact on the transactional strategies of the prosumers. The charging and discharging process of EVs is modeled through Monte Carlo simulations, as reported in Ref. [26]. The dispatch cost associated with EVs can be mathematically expressed as follows:

$$C_{n,t}^{\mathrm{EV}}=\sum_{v=1}^{n_v}\frac{C_v}{L_vE_vh_v}(P_{v,t}^{\mathrm{EV,dis}}-P_{v,t}^{\mathrm{EV,cha}}+S_vd_{v,t}) \tag{9}$$

where $C_{n,t}^{\mathrm{EV}}$ is charging and discharging costs of EV; C_v, L_v, E_v, and h_v represent the battery purchase cost, available number of cycles, capacity, and available discharge limit of the EV, respectively; v is the index of EV; n_v represents the number of EVs available to be dispatched; $P_{v,t}^{\mathrm{EV,dis}}$ and $P_{v,t}^{\mathrm{EV,cha}}$ are discharge and charge power of the vth EV, respectively; S_v is the power consumption per unit distance of the EV; and $d_{v,t}$ is the distance traveled at time t .

3.1.5. Flexible loads (FLs)

FLs exhibit dynamic adaptability, making them capable of adjusting both the magnitude of electricity consumption and the duration of usage. Existing studies commonly employ the elasticity coefficient ε to quantify the responsiveness of these loads to fluctuations in electricity prices.

$$P_{n,t}^{\mathrm{FL}}=P_{n,t,0}^{\mathrm{FL}}\left(\frac{p_{t,\mathrm{DR}}}{p_t}\right)^{-\varepsilon} \tag{10}$$

where $P_{n,t}^{\mathrm{FL}}$ and $P_{n,t,0}^{\mathrm{FL}}$ are FL demand of prosumer n and FL demand before the response, respectively; p_t and $p_{t,\mathrm{DR}}$ are electricity prices before and after the response at time period t, respectively.

The cost of FL scheduling is as follows:

$$C_{n,t}^{\mathrm{FL}}=f_n^{\mathrm{FL}}P_{n,t}^{\mathrm{FL}} \tag{11}$$

where $C_{n,t}^{\mathrm{FL}}$ is scheduling costs of FL and f_n^{FL} is scheduling cost coefficient of FL.

The revenue from the load consumption of prosumers can be represented as follows [27]:

$$C_{n,t}^{\mathrm{L}}=k_n\ln(1+P_{n,t}^{\mathrm{L}}) \tag{12}$$

where $C_{n,t}^{\mathrm{L}}$ represents the benefit of the prosumer to consume electricity $P_{n,t}^{\mathrm{L}}$ for production; $k_n\ln(\cdot)$ is widely used in economics to characterize the decision-making preference process of the prosumer; and k_n represents the decision coefficient of prosumer n.

3.2. The utility function for prosumers participating in P2P trading

The P2P trading market enables prosumers to directly trade electricity and CER without the involvement of a DSO. Prosumers can autonomously control flexible distributed resources, participate in the electricity–carbon coupled market, and dynamically balance energy revenues with carbon-emission costs. The utility function for prosumer n participating in the P2P trading market is represented as follows:

$$\min C_{n,t}^{\mathrm{PR}}=C_{n,t}^{\mathrm{M}}+C_{n,t}^{\mathrm{DG}}+C_{n,t}^{\mathrm{ES}}+C_{n,t}^{\mathrm{EV}}+C_{n,t}^{\mathrm{FL}}+\sum_{m\in\omega_n}C_{\mathrm{nm},t}^{\mathrm{TC}}-C_{n,t}^{\mathrm{T}}-C_{n,t}^{\mathrm{C}}-C_{n,t}^{\mathrm{L}} \tag{13}$$

$$C_{n,t}^{\mathrm{DG}}=C_{n,t}^{\mathrm{G}}+C_{n,t}^{\mathrm{PV}}=\frac{1}{2}a_n^{\mathrm{G}}\left(P_{n,t}^{\mathrm{G}}\right)^2+b_n^{\mathrm{G}}P_{n,t}^{\mathrm{G}}+c_n^{\mathrm{PV}}P_{n,t}^{\mathrm{PV}} \tag{14}$$

s.t. Eqs. (6)–(8)

$$0<P_{n,t}^{\mathrm{G}}<P_{n,t}^{\mathrm{G,max}} \tag{15}$$

$$(1-h_{\mathrm{PV}})P_{n,t}^{\mathrm{PV,max}}<P_{n,t}^{\mathrm{PV}}<P_{n,t}^{\mathrm{PV,max}} \tag{16}$$

$$0\le P_{n,t}^{\mathrm{EV,cha}}\le\eta_{n,t}^{\mathrm{EV}}P_{n,t}^{\mathrm{EV,cha_{max}}} \tag{17}$$

$$0\le P_{n,t}^{\mathrm{EV,dis}}\le(1-\eta_{n,t}^{\mathrm{EV}})P_{n,t}^{\mathrm{EV,dis_{max}}} \tag{18}$$

$$\mathrm{SOC}_n^{\mathrm{EV,min}}\le\mathrm{SOC}_{n,t}^{\mathrm{EV}}\le\mathrm{SOC}_n^{\mathrm{EV,max}} \tag{19}$$

$$P_{n,t}^{\mathrm{FL,min}} < P_{n,t}^{\mathrm{FL}} < P_{n,t}^{\mathrm{FL,max}} \tag{20}$$

$$W_n^{\mathrm{FL}} \le W_{n,0}^{\mathrm{FL}} + \sum_{t=1}^{T}(P_{n,t}^{\mathrm{FL}}) \tag{21}$$

$$P_{n,t}^{\mathrm{G}} + P_{n,t}^{\mathrm{PV}} + P_{n,t}^{\mathrm{M}} + P_{n,t}^{\mathrm{ES,dis}} + P_{n,t}^{\mathrm{EV,dis}} - P_{n,t}^{\mathrm{ES,cha}} - P_{n,t}^{\mathrm{EV,cha}} - \sum_{m\in\omega_n} P_{\mathrm{nm},t}^{\mathrm{T}} - P_{n,t}^{\mathrm{FL}} - P_{n,t}^{\mathrm{L}} = 0 \tag{22}$$

$$D_{n,t}^{0} - \sum_{m\in\omega_n} D_{\mathrm{nm},t}^{\mathrm{T}} \ge R_{n,t} \tag{23}$$

where $C_{n,t}^{\mathrm{PR}}$ is the total cost of prosumer n at time t; $C_{n,t}^{\mathrm{DG}}$ is the electricity generation cost of prosumer n; $C_{\mathrm{nm},t}^{\mathrm{TC}}$ is carbon-coupled network charges for trade nm; $C_{n,t}^{\mathrm{T}}$ and $C_{n,t}^{\mathrm{C}}$ are the electricity and CER traded revenue, respectively; $P_{n,t}^{\mathrm{G,max}}$ is maximum output power of GT; $C_{n,t}^{\mathrm{PV}}$ is the power-generation cost of the PV; c_n^{PV} is the cost factor of PV; $P_{n,t}^{\mathrm{PV,max}}$ and h_{PV} are maximum output power and maximum curtailment rate of PV, respectively; $P_{n,t}^{\mathrm{EV,cha}}$ and $P_{n,t}^{\mathrm{EV,dis}}$ are EV charge and discharge power of prosumer n, respectively; $\eta_{n,t}^{\mathrm{EV}}$ is EV charging states; $P_{n,t}^{\mathrm{EV,cha_{max}}}$ and $P_{n,t}^{\mathrm{EV,dis_{max}}}$ are maximum amount of charge and discharge for EV; respectively; $\mathrm{SOC}_n^{\mathrm{EV,min}}$ and $\mathrm{SOC}_n^{\mathrm{EV,max}}$ are minimum and maximum SOC status of EV, respectively; $\mathrm{SOC}_{n,t}^{\mathrm{EV}}$ is SOC status of EV; $P_{n,t}^{\mathrm{FL,min}}$ and $P_{n,t}^{\mathrm{FL,max}}$ are the minimum and maximum power demands of FL, respectively; $W_{n,0}^{\mathrm{FL}}$ and W_n^{FL} initial demand and final demand of FL, respectively; $P_{\mathrm{nm},t}^{\mathrm{T}}$ and $D_{\mathrm{nm},t}^{\mathrm{T}}$ are the trading electricity and trading CER from prosumer n to prosumer m, respectively; T is the total number of trading periods; $P_{n,t}^{\mathrm{M}}$ is main-grid exchange power of prosumer n ; ω_n is the set of prosumers trading with prosumer n; $D_{n,t}^{0}$ is initial CER of the prosumer n. The first term ($C_{n,t}^{\mathrm{M}}$) in the utility function (Eq. (13)) is the cost of guaranteed trading with the DSO at the time-of-use (TOU) price for buyers and the feed-in-tariff (FiT) price for sellers. Eqs. (6)–(8) and (15)–(21) denote the output power constraint of the prosumer's internal equipment, Eq. (22) denotes the electrical power balance constraint, and Eq. (23) denotes the carbon quota balance constraint. This paper employs a cap-and-trade market for CER trading, leveraging market competition to reflect the scarcity of CER. Within the carbon market, prosumers are required to hold a sufficient number of CER to take responsibility for their carbon emissions. The left-hand side of Eq. (23) represents the CER held by prosumer n, which is equal to the initial CER minus the CER traded in the market. The right-hand side ($R_{n,t}$) of Eq. (23) represents the total carbon emissions generated by the prosumer.

4. The carbon-coupled network charges model for DSO

In this section, we introduce a carbon-coupled network charges model based on the operational conditions of the network. This model encompasses two main components: network operation charges and carbon charges. The DSO can indirectly influence prosumer trading through the implementation of carbon-coupled network charges.

4.1. The DSO optimization model

The DSO employs the AC-OPF [28] methodology for energy scheduling within the distribution grid, with the primary objective being to minimize the DSO's overall operational expenditure. This model is designed to derive network charges that are determined by both power flow and carbon emission flow. The specific DSO model is as follows:

$$\min C_t = \sum_{l\in\Omega} P_{l,t}^{\mathrm{Loss}} p_t^{\mathrm{TOU}} - \sum_{n\in N} C_{n,t}^{\mathrm{M}} - \sum_{i\in N_i} P_{i,t}^{\mathrm{L}} p_t^{\mathrm{TOU}} - \sum_{m\in\omega_n} C_{\mathrm{nm},t}^{\mathrm{TC}} \tag{24}$$

$$\text{s.t} \sum_{l\in\Omega_i^{\mathrm{L+}}} [P_{l,t} - I_{l,t}^2 r_l] + P_{i,t}^{\mathrm{M}} - \sum_{l\in\Omega_i^{\mathrm{L-}}} P_{l,t} - P_{i,t}^{\mathrm{LD}} - G_i V_{i,t}^2 = 0 \tag{25}$$

$$\sum_{l\in\Omega_i^{\mathrm{L+}}} [Q_{l,t} - I_{l,t}^2 x_l] + Q_{i,t}^{\mathrm{M}} - \sum_{l\in\Omega_i^{\mathrm{L-}}} Q_{l,t} - Q_{i,t}^{\mathrm{LD}} + B_i V_{i,t}^2 = 0 \tag{26}$$

$$V_{i,t}^2 - 2(P_{l,t} r_l + Q_{l,t} x_l) + I_{l,t}^2 (r_l^2 + x_l^2) = V_{j,t}^2, \ \forall l \in \Omega_i^{\mathrm{L-}} \tag{27}$$

$$\frac{P_{l,t}^2 + Q_{l,t}^2}{I_{l,t}^2} \le V_{i,t}^2, \forall l \in \Omega_i^{\mathrm{L-}} \tag{28}$$

$$P_{l,t}^2 + Q_{l,t}^2 \le S_l^2, \forall l \in \Omega_i^{\mathrm{L-}} \tag{29}$$

$$(P_{l,t} - I_{l,t}^2 r_l)^2 + (Q_{l,t} - I_{l,t}^2 x_l)^2 \le S_l^2, \forall l \in \Omega_i^{\mathrm{L-}} \tag{30}$$

$$P_{\min}^{\mathrm{M}} \le P_{i,t}^{\mathrm{M}} \le P_{\max}^{\mathrm{M}} \tag{31}$$

$$Q_{i,t} = P_{i,t} \cdot \kappa_i \tag{32}$$

$$\begin{cases} V_{\min} \le V_{i,t} \le V_{\max} \\ 0 \le I_{l,t} \le I_{l,\max} \end{cases} \tag{33}$$

$$\sum_{n\in N} D_{n,t}^{0} = \sum_{n\in N} D_{n,t} \tag{34}$$

where C_t is total operation cost; $P_{l,t}^{\mathrm{Loss}}$ is active power losses of branch l; i and j are indexes of node; p_t^{TOU} is the TOU price; r_l, x_l, B_i, and G_i are circuit parameters of the distribution network, respectively; $P_{l,t}$ and $Q_{l,t}$ are active power and reactive power of branch l, respectively; $P_{i,t}$ and $Q_{i,t}$ are active power and reactive power of node i, respectively; $P_{i,t}^{\mathrm{M}}$ and $Q_{i,t}^{\mathrm{M}}$ are main-grid exchange active power and reactive power, respectively; $P_{i,t}^{\mathrm{LD}}$ and $Q_{i,t}^{\mathrm{LD}}$ are equivalent injected active power and reactive power, respectively; $V_{i,t}$ and $V_{j,t}$ are voltage magnitude of nodes i and j, respectively; $I_{l,t}$ is current of branch l; $P_{i,t}^{\mathrm{M}}$ is main-grid exchange power of node i; $P_{\min}^{\mathrm{M}}$ and $P_{\max}^{\mathrm{M}}$ are minimum and maximum limits of exchange power, respectively; S_l is apparent power of branch l; κ_i is conversion coefficient; $V_{\min}$ and $V_{\max}$ are minimum and maximum limits of node voltage, respectively; $I_{l,\max}$ is upper current limit of line; Ω is the set of branches; $\Omega_i^{\mathrm{L+}}$ and $\Omega_i^{\mathrm{L-}}$ are the set of branches with inflow power and outflow power to node i; N is the set of prosumers; N_i is the set of ordinary load nodes; $P_{i,t}^{\mathrm{L}}$ is the load power; $D_{n,t}$ is final CER of the prosumer n; Eqs. (25) and (26) represent the node active and reactive power balance constraints; Eq. (27) represents the distribution network voltage drop; Eq. (28) represents the second-order cone programming relaxation constraint of the AC power flow equation; Eqs. (29) and (30) represent the line power flow constraint; Eq. (31) represents the substation power generation constraint; and the node reactive power, node voltage, and line current constraints are shown in Eqs. (32) and (33), respectively. The carbon-emission constraints are shown in Eq. (34).

4.2. Carbon-emission responsibility settlement method

Carbon intensity is a pivotal metric in the CEF model, signifying the amount of carbon emissions embodied in a unit of energy flow.

For each node within an energy network, the node carbon intensity (NCI) denotes the average carbon emissions associated with the injected energy flow over a specified period [29]. Consequently, the NCI can be calculated as follows:

$$\rho_{n,t}^{\mathrm{NE}}=\frac{\sum_{l\in\Omega_n^{\mathrm{L}+}}(P_{l,t}-I_{l,t}^2r_l)\cdot\rho_{l,t}^{\mathrm{line}}+P_{n,t}^{\mathrm{G}}\cdot\rho_{n,t}^{\mathrm{G}}+P_{n,t}^{\mathrm{RE}}\cdot\rho_{n,t}^{\mathrm{RE}}}{\sum_{l\in\Omega_n^{\mathrm{L}+}}(P_{l,t}-I_{l,t}^2r_l)+P_{n,t}^{\mathrm{G}}+P_{n,t}^{\mathrm{RE}}} \tag{35}$$

where $\rho_{n,t}^{\mathrm{G}}$ represents the carbon emissions per unit of power generated by the GT, which is intrinsically linked to the thermal unit's operational conditions; $\rho_{n,t}^{\mathrm{NE}}$ is the NCI of node n; $\rho_{n,t}^{\mathrm{RE}}$ represents the carbon emissions for each unit of electricity produced by RES; $P_{n,t}^{\mathrm{G}}$ and $P_{n,t}^{\mathrm{RE}}$ are the output of electricity for GT and RES generators, respectively. $\rho_{l,t}^{\mathrm{line}}$ is defined as the carbon emissions per unit energy flow of branch l at time t.

$$\rho_{l,t}^{\mathrm{line}}\big|_{l\in\Omega_n^{\mathrm{L}-}}=\rho_{n,t}^{\mathrm{NE}} \tag{36}$$

Prosumers' carbon emissions are quantified by the emissions intrinsic to their self-generated power and the carbon emissions associated with the electricity trades, as presented in Eqs. (37)–(39).

$$\rho_{n,t}^{\mathrm{NG}}=\frac{P_{n,t}^{\mathrm{G}}\cdot\rho_{n,t}^{\mathrm{G}}+P_{n,t}^{\mathrm{RE}}\cdot\rho_{n,t}^{\mathrm{RE}}}{P_{n,t}^{\mathrm{G}}+P_{n,t}^{\mathrm{RE}}} \tag{37}$$

$$R_{\mathrm{nm},t}^{\mathrm{T}}=\frac{1}{2}\cdot\rho_{n,t}^{\mathrm{NG}}\cdot P_{\mathrm{nm},t}^{\mathrm{T}} \tag{38}$$

$$R_{\mathrm{nm},t}^{\mathrm{L}}=\frac{1}{2}\cdot\sum_{l\in\Omega}\rho_{l,t}^{\mathrm{line}}\cdot I_{l,t}^2\cdot r_l\frac{P_{l,t}^{\mathrm{T}}}{P_{l,t}} \tag{39}$$

where $\rho_{n,t}^{\mathrm{NG}}$ represents the average carbon intensity of prosumer n; $P_{l,t}^{\mathrm{T}}$ represents power flowing through branch l due to trading nm; $R_{\mathrm{nm},t}^{\mathrm{T}}$ represents the carbon emissions corresponding to the trading nm of electricity; and $R_{\mathrm{nm},t}^{\mathrm{L}}$ represents the equivalent carbon emissions of the line transmission losses. $R_{\mathrm{nm},t}^{\mathrm{T}}$ and $R_{\mathrm{nm},t}^{\mathrm{L}}$ are utilized to calculate the correction of carbon emissions resulting from the trading nm of electrical energy. This approach allows for a more accurate accounting of the carbon footprint associated with energy trades. The total carbon emissions of prosumer n can be represented as follows:

$$R_{n,t}=\begin{cases}R_{n,t}^{\mathrm{NG}}+R_{\mathrm{nm},t}^{\mathrm{L}}-R_{\mathrm{nm},t}^{\mathrm{T}} & n\in N_{\mathrm{s}}\\ R_{n,t}^{\mathrm{NG}}+R_{\mathrm{nm},t}^{\mathrm{L}}+R_{\mathrm{nm},t}^{\mathrm{T}} & n\in N_{\mathrm{b}}\end{cases} \tag{40}$$

where $R_{n,t}^{\mathrm{NG}}$ is the carbon emissions associated with self-generated power; N_{s} and N_{b} are subsets of seller prosumers and buyer prosumers, respectively.

4.3. Carbon-coupled network charges

To facilitate the operation of the electricity–carbon coupled market in an environmentally sustainable and power-grid-compatible manner, we have designed carbon-coupled network charges to guide prosumers in conducting low-carbon and grid-friendly trading. To encourage grid-friendly trading, the carbon-coupled network charges must identify the impact of prosumer trading on the secure operation of the power network. Since the DLMP can reflect the operational status of the network to a certain extent [24], deriving network charges through the DLMP is beneficial for guiding prosumers toward grid-friendly trading. The DLMP is calculated from the power flow calculations and impedance parameters, which are extracted from the operational data of the distribution system.

$$p_{i,t}=A_1\lambda_k+A_2\mu_i+A_3\mu_k+A_4\eta_i^{+}+A_5\eta_i^{-} \tag{41}$$

where A_1–A_5 are the price coefficients; λ_k, μ_i, μ_k, η_i^{+}, and η_i^{-} are dual variables of constraints; $p_{i,t}$ is DLMP at node i.

In the context of electricity trading occurring between disparate nodes within the power system, the DLMP serves as an effective tool for estimating the operational network charges. The corresponding mathematical formulation for this computation is detailed as follows:

$$p_{\mathrm{nm},t}^{\mathrm{O}}=\frac{(p_{s(n),t}-p_{b(m),t})}{2} \tag{42}$$

where $p_{\mathrm{nm},t}^{\mathrm{O}}$ is the operational network charge; $p_{s(n),t}$ is DLMP of prosumer n; $p_{b(m),t}$ is DLMP of prosumer m.

To incentivize prosumers to engage in local trades, this study employs the Thevenin equivalent representation to gauge the electrical distance between participating nodes. The network investment charge $p_{\mathrm{nm},t}^{\mathrm{I}}$ can be calculated utilizing the equation provided in Eq. (43).

$$p_{\mathrm{nm},t}^{\mathrm{I}}=p^{\mathrm{dis}}Z_{i,j}^{\mathrm{Th}}/2 \tag{43}$$

where p^{dis} is distance unit cost; $Z_{i,j}^{\mathrm{Th}}$ is the Thevenin electrical distance.

Thus, the network charges associated with network operations can be determined as follows:

$$C_{\mathrm{nm},t}^{\mathrm{T}}=\left(p_{\mathrm{nm},t}^{\mathrm{O}}+p_{\mathrm{nm},t}^{\mathrm{I}}\right)\cdot P_{\mathrm{nm},t}^{\mathrm{T}} \tag{44}$$

where $C_{\mathrm{nm},t}^{\mathrm{T}}$ is network charges associated with network operations.

Accurately calculating the carbon-emission costs during prosumer trading is crucial for promoting low-carbon trading. Based on the aforementioned carbon footprint tracking methods, quantifying carbon-emission costs can economically steer prosumers' trading. A carbon-pricing mechanism can be employed to calculate the carbon-emission costs for prosumers, with severe economic penalties being imposed for excess carbon emissions.

Currently, carbon-pricing mechanisms in the carbon market predominantly consist of two approaches: the conventional fixed price and tiered pricing. However, the static fixed price fails to cater to low-emission generators and inadequately penalizes high emitters, thereby disincentivizing low-carbon transitions [30]. When their emissions exceed their allotted rights, prosumers must purchase additional allowances from the market, incurring substantial penalties. Conversely, when their emissions fall below their allotment, prosumers can exploit the market to sell surplus allowances, reaping benefits that are directly proportional to the excess and the price differential. The greater the reduction in emissions, the more allowances they can sell, thereby enhancing their economic benefits. Therefore, employing a tiered pricing approach to derive network charges can effectively incentivize prosumers to decarbonize.

$$F^{\mathrm{C}}(\delta)=\begin{cases}c_{\mathrm{CE},1}\delta_1+c_{\mathrm{CE},2}(\delta-\delta_1) & \delta<-\delta_1\\ c_{\mathrm{CE},1}\delta & -\delta_1\le\delta<\delta_1\\ c_{\mathrm{CE},1}\delta_1+c_{\mathrm{CE},2}(\delta-\delta_1) & \delta_1\le\delta<\delta_2\\ c_{\mathrm{CE},1}\delta_1+c_{\mathrm{CE},2}(\delta_2-\delta_1)+c_{\mathrm{CE},3}(\delta-\delta_2) & \delta_2\le\delta<\delta_3\\ c_{\mathrm{CE},1}\delta_1+c_{\mathrm{CE},2}(\delta_2-\delta_1)+c_{\mathrm{CE},3}(\delta_3-\delta_2)+c_{\mathrm{CE},4}(\delta-\delta_3) & \delta_3\le\delta<\delta_4\end{cases} \tag{45}$$

where δ is the net carbon emissions; $F^{\mathrm{C}}(\cdot)$ is network charges associated with carbon-emission ; $c_{\mathrm{CE},1}$–$c_{\mathrm{CE},4}$ are the unit cost of stepped carbon emissions; and δ_1–δ_4 are the boundary of the carbon-emission price range.

Consequently, by taking into account the specific carbon emissions of the aforementioned prosumers and the corresponding carbon-pricing mechanisms, the carbon-coupled network charges can be derived:

$$C^{\mathrm{TC}}_{\mathrm{nm},t}(P^{\mathrm{T}}_{\mathrm{nm},t}) = C^{\mathrm{T}}_{\mathrm{nm},t}(P^{\mathrm{T}}_{\mathrm{nm},t}) + F^{\mathrm{C}}_{\mathrm{nm},t}(R^{\mathrm{EX}}_{n,t}) \tag{46}$$

where $F^{\mathrm{C}}_{\mathrm{nm},t}(\cdot)$ is canbon-related network charges for trade nm; $R^{\mathrm{EX}}_{n,t}$ is excess carbon emissions of prosumer n.

5. Algorithm solving

5.1. A clearing method for the P2P coupled market

In this paper, the ADMM is deployed to address the complex task of clearing P2P trading in the coupled market. The ADMM ingeniously decomposes the original global challenge into a series of smaller, more manageable local sub-problems, which can then be effectively solved in parallel. By coordinating these sub-problems, the algorithm strives to achieve the optimal solution for the market [31]. Its methodology involves treating unoptimized variables as constants during the iterative process and utilizing the results from the previous iteration until the desired level of accuracy is attained.

Based on the ADMM algorithm, the joint trading mechanism in this paper can be modified to

$$\begin{cases} \min F^{\mathrm{PR}}_n = \sum\limits_{t\in T} C^{\mathrm{PR}}_{n,t} \\ \text{s.t. Eqs. (6)} - \text{(8)}, \text{Eqs. (15)} - \text{(23)} \end{cases} \tag{47}$$

where F^{PR}_n is the total cost for prosumer n.

$\boldsymbol{X}^{\mathrm{PR}}_n = [P^{\mathrm{DG}}_{n,t}, P^{\mathrm{FL}}_{n,t}, P^{\mathrm{T}}_{n,t}, P^{\mathrm{M}}_{n,t}, P^{\mathrm{ES}}_{n,t}, D^{\mathrm{T}}_{n,t}]$ is the decision-making variable for prosumer n, where $P^{\mathrm{T}}_{n,t}$ and $D^{\mathrm{T}}_{n,t}$ are the electricity and CER traded of prosumer n, respectively; $P^{\mathrm{DG}}_{n,t}$ is the electricity generation of prosumer n.

Set up $\boldsymbol{x}_n = [x^{\mathrm{T}}_n, x^{\mathrm{C}}_n]^{\mathrm{T}}$, $x^{\mathrm{T}}_n = P^{\mathrm{T}}_{\mathrm{nm},t}$, $x^{\mathrm{C}}_n = D^{\mathrm{T}}_{\mathrm{nm},t}$; introduce the auxiliary variables $\boldsymbol{z}_n = [z^{\mathrm{Tk}}_n, z^{\mathrm{Ck}}_n]^{\mathrm{T}}$, $z^{\mathrm{Tk}}_n = -P^{\mathrm{T}}_{\mathrm{mn},t}$, $z^{\mathrm{Ck}}_n = -D^{\mathrm{T}}_{\mathrm{mn},t}$, where $\boldsymbol{x}_n$ and $\boldsymbol{z}_n$ are trading variables and auxiliary variables, respectively; x^{T}_n and x^{C}_n are the electricity and CER trading variables; z^{Tk}_n and z^{Ck}_n are the electricity and CER auxiliary variables; $P^{\mathrm{T}}_{\mathrm{mn},t}$ and $D^{\mathrm{T}}_{\mathrm{mn},t}$ are the trading electricity and trading CER from prosumer m to prosumer n, respectively. Then:

$$\boldsymbol{x}_n - \boldsymbol{z}_n = 0 \tag{48}$$

The augmented Lagrange function L_ρ of the given problem is as follows:

$$\begin{aligned} L_\rho(\boldsymbol{x}_n, \boldsymbol{z}_n, \lambda_{\mathrm{nm},t}, \pi_{\mathrm{nm},t}) &= F^{\mathrm{PR}}_n(\boldsymbol{x}_n) + g(\boldsymbol{z}_n) \\ &+ \sum_{m=1,m\neq n}^{N} \left[\lambda^k_{\mathrm{nm},t}\left(x^{\mathrm{T}}_n - z^{\mathrm{Tk}}_n\right) + \tfrac{\rho}{2}\| x^{\mathrm{T}}_n - z^{\mathrm{Tk}}_n \|_2^2\right] \\ &+ \sum_{m=1,m\neq n}^{N} \left[\pi^k_{\mathrm{nm},t}\left(x^{\mathrm{C}}_n - z^{\mathrm{Ck}}_n\right) + \tfrac{\chi}{2}\| x^{\mathrm{C}}_n - z^{\mathrm{Ck}}_n \|_2^2\right] \end{aligned} \tag{49}$$

where $\lambda^k_{\mathrm{nm},t}$ and $\pi^k_{\mathrm{nm},t}$ are consensus constraints, which are also defined as P2P prices for trading energy and CER, respectively; k is the number of iterations; $g(\boldsymbol{z}_n)$ is the indicator function, where $g(\boldsymbol{z}_n) = 0$ when the variable $\boldsymbol{z}_n$ satisfies the feasible domain and $g(\boldsymbol{z}_n) = \infty$ when the feasible domain is not satisfied; and ρ, χ are the penalty factors.

Therefore, the original problem is broken down into

$$\begin{cases} \boldsymbol{x}^{k+1}_n = \arg\min_x L_\rho(\boldsymbol{x}^k_n, \boldsymbol{z}^k_n, \lambda^k_{\mathrm{nm},t}, \pi^k_{\mathrm{nm},t}) \\ \boldsymbol{z}^{k+1}_n = \arg\min_z L_\rho(\boldsymbol{x}^{k+1}_n, \boldsymbol{z}^k_n, \lambda^k_{\mathrm{nm},t}, \pi^k_{\mathrm{nm},t}) \\ \lambda^{k+1}_{\mathrm{nm},t} = \lambda^k_{\mathrm{nm},t} - \rho(P^{\mathrm{T}(k+1)}_{\mathrm{nm},t} + P^{\mathrm{T}(k+1)}_{\mathrm{mn},t})/2 \\ \pi^{k+1}_{\mathrm{nm},t} = \pi^k_{\mathrm{nm},t} - \chi(D^{\mathrm{T}(k+1)}_{\mathrm{nm},t} + D^{\mathrm{T}(k+1)}_{\mathrm{mn},t})/2 \end{cases} \tag{50}$$

$$\begin{cases} \mathrm{re}^{k+1}_{n,t} = \sum\limits_{m\in\omega_n}\left(P^{\mathrm{T}(k+1)}_{\mathrm{nm},t} + P^{\mathrm{T}(k+1)}_{\mathrm{mn},t}\right) \\ \mathrm{rs}^{k+1}_{n,t} = \sum\limits_{m\in\omega_n}\left(P^{\mathrm{T}(k+1)}_{\mathrm{nm},t} - P^{\mathrm{T}(k)}_{\mathrm{nm},t}\right) \end{cases} \tag{51}$$

$$\begin{cases} \mathrm{ce}^{k+1}_{n,t} = \sum\limits_{m\in\omega_n}\left(D^{\mathrm{T}(k+1)}_{\mathrm{nm},t} + D^{\mathrm{T}(k+1)}_{\mathrm{mn},t}\right) \\ \mathrm{cs}^{k+1}_{n,t} = \sum\limits_{m\in\omega_n}\left(D^{\mathrm{T}(k+1)}_{\mathrm{nm},t} - D^{\mathrm{T}(k)}_{\mathrm{nm},t}\right) \end{cases} \tag{52}$$

where $P^{\mathrm{T}(k+1)}_{\mathrm{nm},t}$ and $D^{\mathrm{T}(k+1)}_{\mathrm{nm},t}$ are trading power and trading CER from prosumer n to prosumer m in the $(k+1)$th iteration; $P^{\mathrm{T}(k+1)}_{\mathrm{mn},t}$ and $D^{\mathrm{T}(k+1)}_{\mathrm{mn},t}$ are trading power and trading CER from prosumer m to prosumer n in the $(k+1)$th iteration; $\mathrm{re}^{k+1}_{n,t}$ and $\mathrm{ce}^{k+1}_{n,t}$ are primal residuals; $\mathrm{rs}^{k+1}_{n,t}$ and $\mathrm{cs}^{k+1}_{n,t}$ are dual residuals.

Given that the objective function of the P2P coupled trading market exhibits strict convexity and closedness, the ADMM algorithm's efficacy and convergence are inherently assured [32]. The algorithm's convergence is governed by a well-defined convergence criterion, which can be mathematically expressed as follows:

$$\begin{cases} \sum\limits_{n\in N}\left(\| \mathrm{re}^{k+1}_{n,t} \|_2 + \| \mathrm{rs}^{k+1}_{n,t} \|_2\right) \le \varepsilon_1 \\ \sum\limits_{n\in N}\left(\| \mathrm{ce}^{k+1}_{n,t} \|_2 + \| \mathrm{cs}^{k+1}_{n,t} \|_2\right) \le \varepsilon_2 \end{cases} \tag{53}$$

where ε_1 and ε_2 are convergence thresholds.

In the ADMM, convergence is achievable with any fixed penalty factor; however, the rate of convergence is significantly influenced by this factor. An imprecise selection of the penalty factor ρ may necessitate a higher number of iterations for convergence [33]. Based on the algorithm's inherent principles, the following observations can be drawn: As ρ increases, the primal residual diminishes, concurrently causing an increase in the dual residual. Conversely, when ρ is reduced, the primal residual escalates, while the dual residual decreases. Eq. (53) reveals that both residuals must be very small at the point of convergence. To address this, a residual coefficient τ is introduced to dynamically update penalty factors, striking a balance between the primal and dual residuals and thereby increasing the convergence speed.

$$\rho^{k+1} = \begin{cases} \tau_\rho \rho^k & \| \mathrm{re}^k_{n,t} \|_2 > o_{\mathrm{e}} \| \mathrm{rs}^k_{n,t} \|_2 \\ \rho^k/\tau_\rho & \| \mathrm{rs}^k_{n,t} \|_2 > o_{\mathrm{e}} \| \mathrm{re}^k_{n,t} \|_2 \\ \rho^k & \text{others} \end{cases} \tag{54}$$

$$\chi^{k+1} = \begin{cases} \tau_{\mathrm{c}} \chi^k & \| \mathrm{ce}^k_{n,t} \|_2 > o_{\mathrm{c}} \| \mathrm{cs}^k_{n,t} \|_2 \\ \chi^k/\tau_{\mathrm{c}} & \| \mathrm{cs}^k_{n,t} \|_2 > o_{\mathrm{c}} \| \mathrm{ce}^k_{n,t} \|_2 \\ \chi^k & \text{others} \end{cases} \tag{55}$$

where o_{e} and o_{c} are proportionality coefficients; τ_ρ and τ_{c} are residual coefficients.

5.2. Bi-level model solution algorithm

In iteratively solving the bi-level model of the DSO and P2P market, the question of how to ensure the convergence of the bi-level interaction is a difficult point. Therefore, this paper proposes an improved bisection method to solve the bi-level interaction

convergence problem based on Ref. [34]; the specific process is shown in Algorithm 1.

Algorithm 1. The improved bisection iterative method.

Initialization: The number of iterations is z, the trading energy of prosumer n is $P_{n,t}^{\mathrm{T}(z-1)}$, and the initial operation interval is $\left[P_{n,t}^{\min}, P_{n,t}^{\max}\right]$
While not converged **do**
  Let $P_{n,t}^{\mathrm{avg}} = (P_{n,t}^{\min} + P_{n,t}^{\max})/2$, $z = z + 1$
  Solve the prosumer model with the constraints $P_{n,t}^{\min} \le P_{n,t}^{\mathrm{avg}} \le P_{n,t}^{\max}$, and the trading energy $P_{n,t}^{\mathrm{T}(z)}$ is obtained based on the optimization of network charges in the last iteration
  Utilize the optimization of DSO and CEF models to calculate carbon-coupled network charges. Verify trading results compliance with network constraints
  if meets network constraints and satisfies convergence criterion
    Terminate the iteration
  else if $P_{n,t}^{\mathrm{T}(z)} < P_{n,t}^{\mathrm{avg}}$ then
    Update the upper bound of the interval $P_{n,t}^{\max} = (P_{n,t}^{\max} + P_{n,t}^{\mathrm{avg}})/2$
  else if $P_{n,t}^{\mathrm{T}(z)} > P_{n,t}^{\mathrm{avg}}$ then
    Update the lower bound of the interval $P_{n,t}^{\min} = (P_{n,t}^{\min} + P_{n,t}^{\mathrm{avg}})/2$
  end if
End while

The core principle of the improved bisection lies in its iterative refinement of the energy trading interval, ensuring that it continually encircles the optimal solution by adjusting the lower or upper bounds in each iteration. This approach guarantees convergence within a finite number of iterations.

The proposed bi-level interactive optimization method employing the improved bisection method is outlined as follows: At the upper level, operators perform security assessments based on the outcomes of P2P market trading. If the convergence criteria are satisfied, the trading results are outputted; otherwise, carbon-coupled network charges are calculated to guide trading in the electricity–carbon coupled market. At the lower level, prosumers adjust their trading strategies based on the network charges and submit stable trading results to DSOs for validation. The bi-level model continues to interact and iterate, with the improved bisection method ensuring the convergence of the iterative process. The specific implementation process is illustrated in Fig. 2.

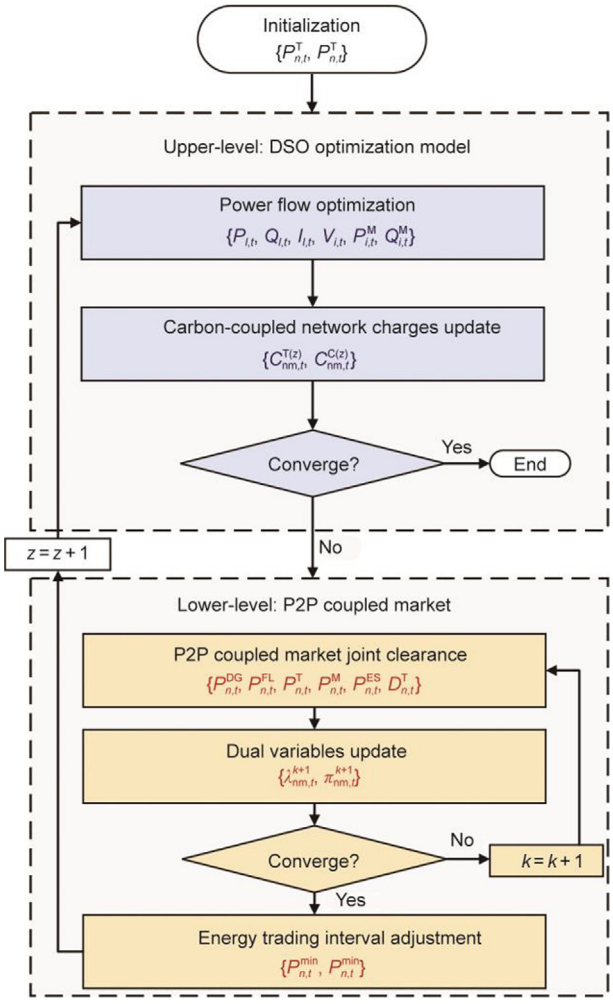

Fig. 2. Flowchart of the bi-level interactive optimization method.

6. Case study

6.1. Case description

In this paper, a modified Institute of Electrical and Electronics Engineers (IEEE) 33-bus system is employed to validate the proposed model and algorithm, as shown in Fig. 3. The system, which includes 33 buses, features a mix of prosumer and conventional consumer buses. The prosumers are equipped with various distributed resources, including GTs, PVs, ES, and FLs.

The main input data for the day-ahead market is shown in Fig. 4, including the 24 h typical load and distributed power generation.

Four cases are employed to evaluate the economic and low-carbon performance of the DSO–prosumers bi-level interactive framework, as well as the efficacy of the proposed algorithm.

Case 1: No P2P trading.

Case 2: Only P2P electricity trading, no carbon market participation is considered.

Case 3: Electricity–carbon coupled P2P trading market without considering carbon-coupled network charges.

Case 4: Electricity–carbon coupled P2P trading market, considering carbon-coupled network charges.

6.2. Trading results of the electricity–carbon coupled P2P trading market

The prosumers participating in the proposed P2P coupled market act in self-interest, making autonomous decisions regarding the trading price and quantity of electricity based on considerations of energy trading and carbon emissions. The remaining unallocated electricity is centrally dispatched by the DSO, with the DSO determining the electricity prices. Fig. 5 presents the trading prices of prosumers across a 24 h period, where the blue portion of the figure delineates the specific range of prosumer trading prices. It is observed that all trading prices fall between the FiT and the TOU electricity price. This indicates that, in the energy trading market, sellers can offer energy at prices above the FiT at which

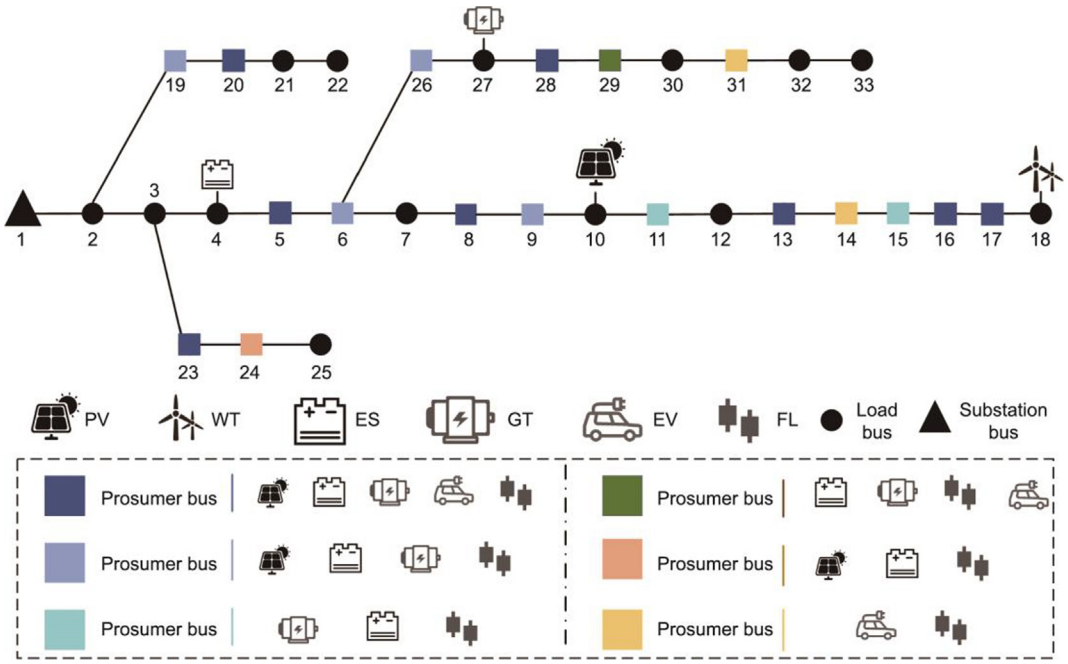

Fig. 3. The IEEE 33-bus system.

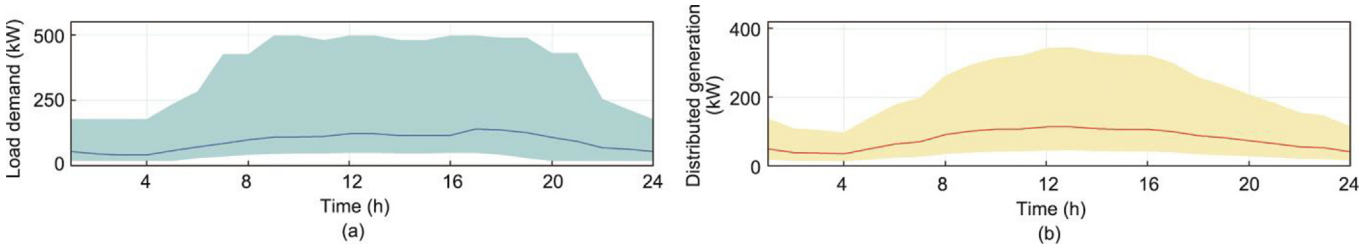

Fig. 4. Forecast profiles of the typical load and distributed power generation over 24 h. (a) Load demand; (b) distributed generation.

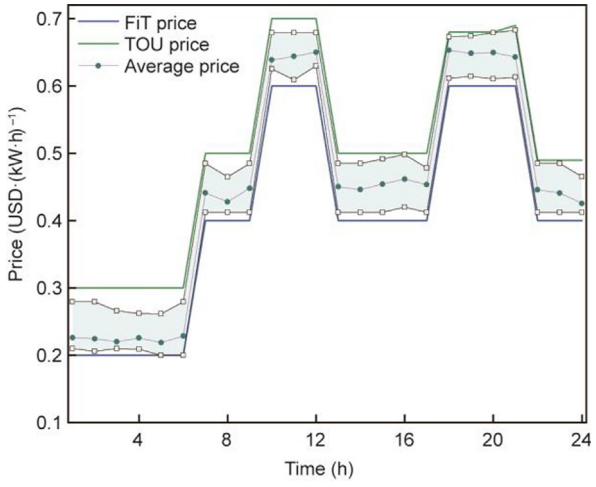

Fig. 5. Hourly P2P energy trading prices in the energy trading market.

the DSO purchases energy, while buyers can secure energy at prices lower than the DSO's TOU price.

Furthermore, to better demonstrate the P2P market's potential to enhance prosumers' economic benefits, we compare the total prosumer revenues in Cases 1 and 4, as shown in Fig. 6. It becomes evident that, when prosumers exclude P2P energy trading, their earnings are limited to interactions with DSOs, resulting in significantly reduced profits. By engaging in electricity market trading, prosumers can capitalize on higher selling prices and lower buying costs, thereby enhancing their financial gains. The surge in the prosumers' electricity purchase cost between 17:00 and 21:00 stems from the higher electricity demand exceeding the generated supply during this period, which drives up energy prices. Prosumers can enhance their profits by negotiating trading through the energy market. Although prosumers incur certain carbon-emission costs when considering carbon trading, their total revenue remains higher than if they did not participate. This is because the proportion of carbon-emission costs is relatively small compared with the increased revenue from electricity trading.

Fig. 7 illustrates the trading energy and corresponding average trading prices in the P2P trading market. As observed in Fig. 7, within the same price range, the higher the trading volume between prosumers, the lower the average trading price. This phenomenon occurs because the net power output of prosumers is positive, indicating a supply surplus. Consequently, buying prosumers, guided by economic costs, opt to purchase electricity from sellers offering lower prices, as demonstrated during the 9:00–11:00 AM period. The significant trading volume at 21:00 is attributed to the reduction in PV generation, leading to a decrease in energy supply within the market. As a result, the majority of prosumers purchase energy from high-carbon prosumers to compensate for their energy shortfall.

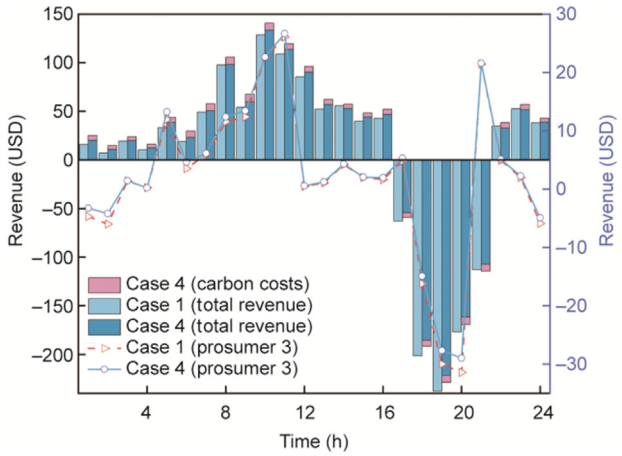

Fig. 6. A comparison of prosumer benefit results over 24 h in Cases 1 and 4.

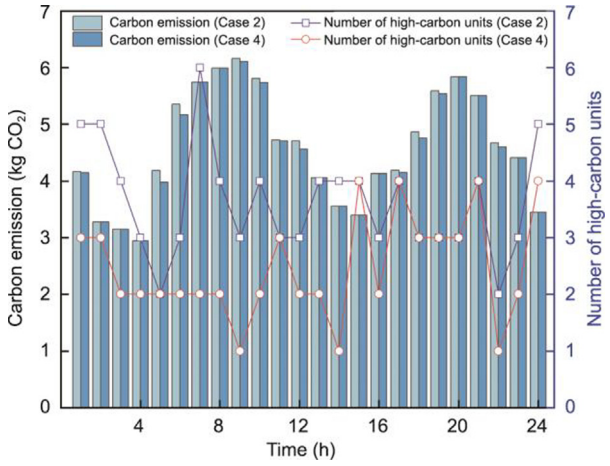

Fig. 8. Comparison of market carbon emissions in Cases 2 and 4.

6.3. The impact of the bi-level interactive model on carbon emissions

Comparing Cases 2 and 4 reveals that, when just the electric energy trading among prosumers are taken into account, the overall carbon emissions and the count of high-carbon-emitting prosumers participating in the trade surpass those in the coupled trading scenario, as shown in Fig. 8. This is due to the fact that, when energy trading is the primary focus, prosumers with a higher proportion of fuel-based units experience lower production costs compared with those with a lower proportion. In the context of the P2P coupled market, prosumers must consider not only the implications of energy trading but also the carbon-emission costs. Consequently, the competitiveness of prosumers with abundant RES is enhanced in this coupled market, leading to a reduction in total carbon emissions.

Fig. 9 presents the prosumer trading for Cases 2 and 4. In the P2P coupled market, the electric energy trading volume of high-carbon prosumers witnesses a decline or even a withdrawal from the market. Simultaneously, the market participation priority of low-carbon prosumers increases, resulting in a corresponding rise in energy trading volume. This presents the effectiveness of the

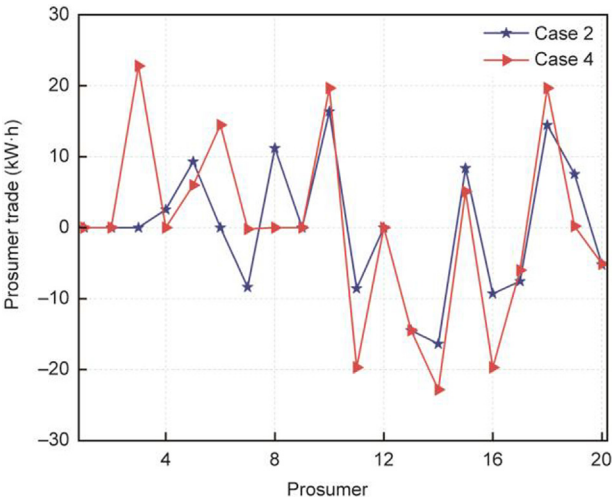

Fig. 9. Comparison of prosumer trading results in Cases 2 and 4.

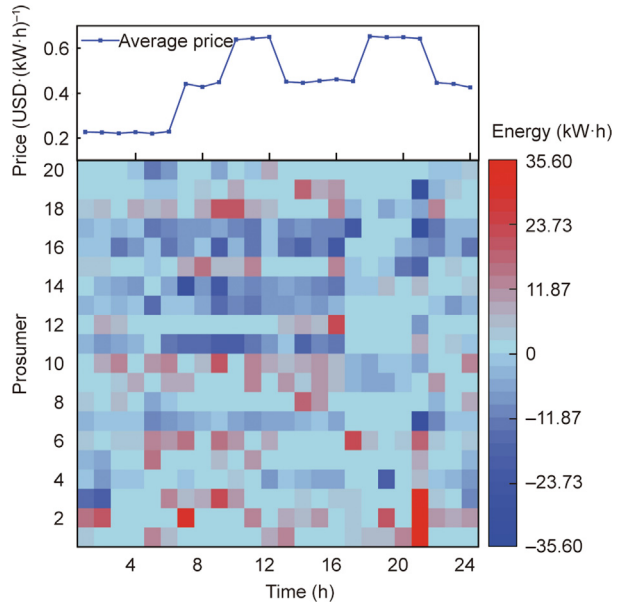

Fig. 7. Trading activity of prosumers over 24 h.

electricity–carbon coupled P2P trading market in carbon-emission reduction.

6.4. The impact of carbon-coupled network charges on network operations

To illustrate the network charge's influence on the P2P trading network's friendliness in the electricity–carbon coupled market, we compare the distribution line loads and node voltages between Cases 3 and 4, as depicted in Fig. 10. As evident from the figure, the line load in Case 4, which accounts for network charges, significantly drops compared with that in Case 3, where such charges are disregarded. The network charges can reflect the operational expenses of the power grid, and prosumers are required to cover the usage costs associated with P2P trading, including congestion fees. This incentivizes prosumers to adhere to network constraints, thereby minimizing the likelihood of congestion and keeping the node voltages within a narrower range, which ensures grid stability. Consequently, network charges play an important role in mitigating congestion risks and maintaining the secure operation of the system.

6.5. The impact of RES penetration on the bi-level interactive model

In order to explore the impact of RES penetration on the bi-level interactive model, the problems that may be faced in the process of the decarbonization of distribution networks are discussed. This

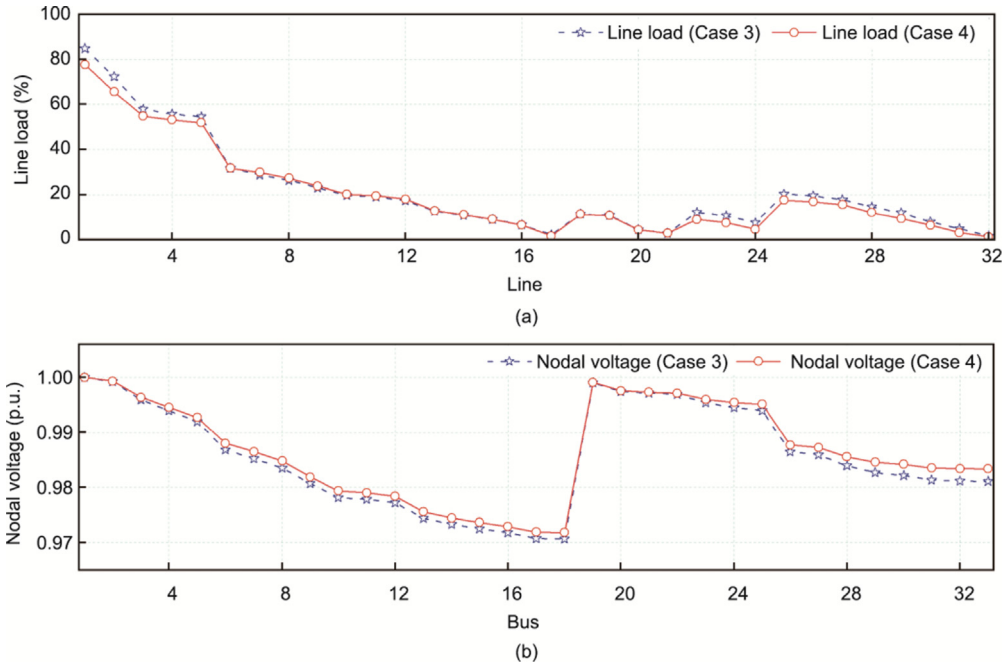

Fig. 10. (a) Distribution line loading and (b) nodal voltage magnitudes under Cases 3 and 4. p.u.: per unit.

discussion reflects the fact that the trading volume, trading price of electric energy, and carbon-emission trading price are affected by the penetration rate of RES.

As depicted in Fig. 11, a rise in RES penetration from 70% to 160% leads to an approximate 12% increase in electricity trading prices among prosumers, while carbon-emission prices undergo a corresponding decrease of around 15%. In a market dominated by fossil fuel power plants, the scarcity of CER intensifies competition among prosumers, driving up CER prices. Prosumers must compete more intensely for the limited CER in the market to reduce their carbon-emission costs, thereby driving up the price of CER. At the same time, power-producing prosumers may lower their electricity selling prices to sell energy at a lower cost, effectively transferring carbon emissions to the electricity buyers in the form of a flow, in order to reduce their own carbon emissions during settlement. With the energy transition and the increasing penetration of renewable energy, the market's CER increase, the cost of producing electricity for prosumers rises, the selling price of electricity increases, and the price of CER decreases.

As the penetration rate of RES increases, the influence of the carbon market on the electricity market diminishes. Prosumers may find it more cost-effective to purchase a small proportion of energy generated from fossil fuels and balance their energy supply through their own dispatch, leading to a slight decrease in energy trading volume. To avoid incurring additional carbon-emission costs, prosumers are inclined to produce or purchase renewable energy. Therefore, the proposed electricity–carbon coupled P2P trading market can facilitate the energy transition in the distribution network.

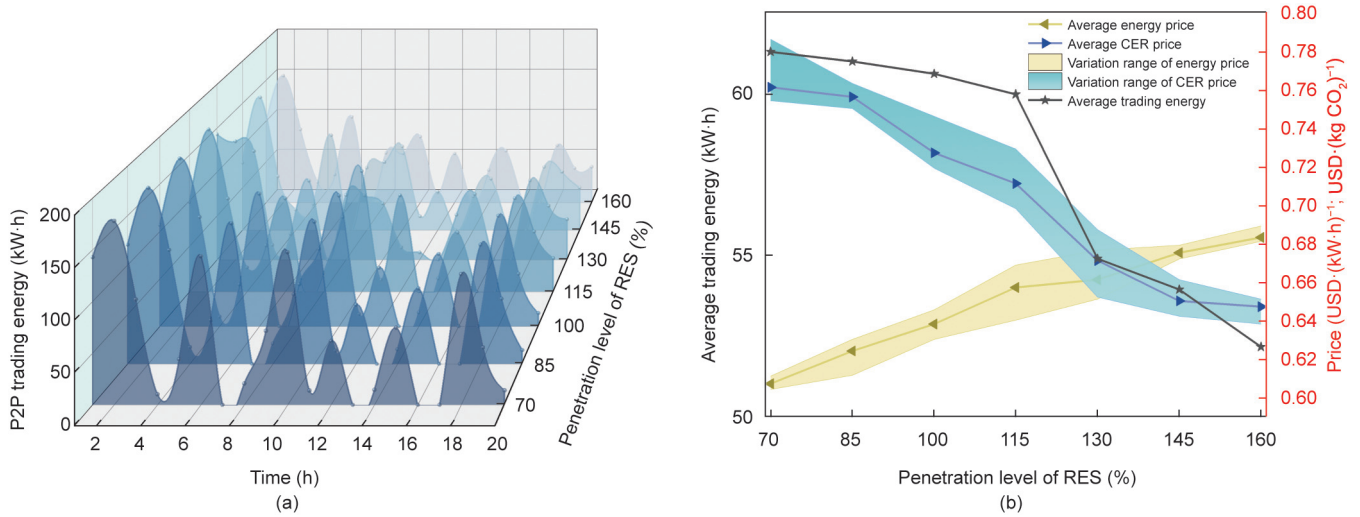

Fig. 11. P2P trading energy, energy trading price, and CER trading price for different RES penetration levels. (a) P2P trading energy; (b) energy and CER trading price.

7. Conclusions

This paper proposes a carbon-coupled network charge-guided bi-level interactive optimization method between the DSO and prosumers. To enforce safe and low-carbon operation in distribution networks, the framework incorporates a carbon-coupled network charges mechanism that adjusts trading among prosumers. The adaptive ADMM algorithm facilitates market clearing, while the improved bisection method ensures convergence in the bi-level interaction, enabling prosumers to interact effectively while preserving their privacy and minimizing computational demands.

This case study validates the efficacy of the proposed bi-level interactive model. First, the model achieves optimal electricity–carbon P2P trading surpassing traditional market schemes in both economic benefits and carbon-emission reduction. Second, the introduced carbon-emission responsibility settlement method quantifies the carbon emissions of different nodes, ensuring the accurate apportionment of carbon emissions. Third, the carbon-coupled network charges proposed by the model effectively guides prosumers to adjust their trading strategies, facilitating energy trading that is proximity-based, network-friendly, and low-carbon oriented, while maintaining line loadings and node voltages within safe operational limits. Notably, the incentive effect of the carbon-coupled network charges becomes more pronounced with a decrease in the penetration rate of RES.

It is important to note that the uncertainties associated with renewable energy generation and load demand may lead to fluctuations in the trading behavior of prosumers, potentially resulting in economic losses, which would be considered and integrated in the future risk-averse P2P trading strategies studies.

CRediT authorship contribution statement

Huangqi Ma: Writing – original draft, Conceptualization. **Yue Xiang:** Writing – review & editing. **Alexis Pengfei Zhao:** Writing – review & editing. **Shuangqi Li:** Writing – review & editing. **Junyong Liu:** Writing – review & editing.

Declaration of competing interest

The authors declare that they have no known competing financial interests or personal relationships that could have appeared to influence the work reported in this paper.

Acknowledgments

This work was supported by Institutional Research Fund from Sichuan University (0-1 Innovation Research Project, 2023SCUH0002), the Sichuan Science and Technology Program (2024YFHZ0312), the Chengdu Science and Technology Program (2024YF0600012HZ), the National Natural Science Foundation of China (U2166211 and 52177103).

References

[1] Li Y, Ding Y, He S, Hu F, Duan J, Wen G, et al. Artificial intelligence-based methods for renewable power system operation. Nat Rev Electr Eng 2024;1(3):163–79.
[2] Li Y, Yu C, Shahidehpour M, Yang T, Zeng Z, Chai T. Deep reinforcement learning for smart grid operations: algorithms, applications, and prospects. P IEEE 2023;111(9):1055–96.
[3] Wu C, Chen X, Hua H, Yu K, Gan L, Shen J, et al. Peer-to-peer energy trading optimization for community prosumers considering carbon cap-and-trade. Appl Energy 2024;358:122611.
[4] Cui S, Wang YW, Shi Y, Xiao JW. An efficient peer-to-peer energy-sharing framework for numerous community prosumers. IEEE T Ind Inform 2019;16 (12):7402–12.
[5] Yao H, Xiang Y, Hu S, Wu G, Liu J. Optimal prosumers' peer-to-peer energy trading and scheduling in distribution networks. IEEE T Ind Appl 2022;58 (2):1466–77.
[6] Mu C, Ding T, Zhu S, Han O, Du P, Li F. A decentralized market model for a microgrid with carbon emission rights. IEEE T Smart Grid 2022;14 (2):1388–402.
[7] Lu Z, Bai L, Wang J, Wei J, Xiao Y, Chen Y. Peer-to-peer joint electricity and carbon trading based on carbon-aware distribution locational marginal pricing. IEEE T Power Syst 2022;38(1):835–52.
[8] Morstyn T, Teytelboym A, McCulloch MD. Bilateral contract networks for peer-to-peer energy trading. IEEE T Smart Grid 2018;10(2):2026–35.
[9] Anoh K, Maharjan S, Ikpehai A, Zhang Y, Adebisi B. Energy peer-to-peer trading in virtual microgrids in smart grids: a game-theoretic approach. IEEE T Smart Grid 2019;11(2):1264–75.
[10] Yao H, Xiang Y, Gu C, Liu J. Peer-to-peer coupled trading of energy and carbon emission allowance: a stochastic game-theoretic approach. IEEE Internet Things 2024;11(14):24364–75.
[11] Zhong W, Xie K, Liu Y, Yang C, Xie S. Multi-resource allocation of shared energy storage: a distributed combinatorial auction approach. IEEE T Smart Grid 2020;11(5):4105–15.
[12] Haggi H, Sun W. Multi-round double auction-enabled peer-to-peer energy exchange in active distribution networks. IEEE T Smart Grid 2021;12 (5):4403–14.
[13] Song M, Sun W, Wang Y, Shahidehpour M, Li Z, Gao C. Hierarchical scheduling of aggregated TCL flexibility for transactive energy in power systems. IEEE T Smart Grid 2019;11(3):2452–63.
[14] Wei C, Wang Y, Shen Z, Xiao D, Bai X, Chen H. AUQ-ADMM algorithm-based peer-to-peer trading strategy in large-scale interconnected microgrid systems considering carbon trading. IEEE Syst J 2023;17(4):6248–59.
[15] Xiang Y, Qing G, Fang M, Li Z, Yao H, Liu J, et al. A carbon emission allowance bargaining model for energy transactions among prosumers. IEEE T Power Syst 2024;39(4):6095–8.
[16] Wang Y, Qiu J, Tao Y, Zhang X, Wang G. Low-carbon oriented optimal energy dispatch in coupled natural gas and electricity systems. Appl Energy 2020;280:115948.
[17] Cheng Y, Zhang N, Lu Z, Kang C. Planning multiple energy systems toward low-carbon society: a decentralized approach. IEEE T Smart Grid 2018;10 (5):4859–69.
[18] Wang Y, Qiu J, Tao Y, Zhao Z. Carbon-oriented operational planning in coupled electricity and emission trading markets. IEEE T Power Syst 2020;35 (4):3145–57.
[19] Cheng Y, Zhang N, Wang Y, Yang J, Kang C, Xia Q. Modeling carbon emission flow in multiple energy systems. IEEE T Smart Grid 2018;10(4):3562–74.
[20] Cheng Y, Zhang N, Zhang B, Kang C, Xi W, Feng M. Low-carbon operation of multiple energy systems based on energy–carbon integrated prices. IEEE T Smart Grid 2019;11(2):1307–18.
[21] Ullah MH, Park JD. Peer-to-peer energy trading in transactive markets considering physical network constraints. IEEE T Smart Grid 2021;12 (4):3390–403.
[22] Ruan H, Gao H, Gooi HB, Liu J. Active distribution network operation management integrated with P2P trading. Appl Energy 2022;323:119632.
[23] Baroche T, Pinson P, Latimier RLG, Ahmed HB. Exogenous cost allocation in peer-to-peer electricity markets. IEEE T Power Syst 2019;34(4):2553–64.
[24] Yao H, Xiang Y, Liu J. Virtual prosumers' P2P transaction based distribution network expansion planning. IEEE T Power Syst 2024;39(1):1044–57.
[25] Chen Z, Zhang Y, Ji T, Cai Z, Li L, Xu Z. Coordinated optimal dispatch and market equilibrium of integrated electric power and natural gas networks with P2G embedded. J Mod Power Syst Cle 2018;6(3):495–508.
[26] Cui S, Wang YW, Li C, Xiao JW. Prosumer community: a risk aversion energy sharing model. IEEE T Sustain Energy 2019;11(2):828–38.
[27] Li J, Ge S, Liu H, Yu Q, Zhang S, Wang C, et al. An electricity and carbon trading mechanism integrated with TSO–DSO–prosumer coordination. Appl Energy 2024;356:122328.
[28] Kim J, Dvorkin Y. A P2P-dominant distribution system architecture. IEEE T Power Syst 2019;35(4):2716–25.
[29] Kang C, Zhou T, Chen Q, Xia Q, Ji Z. Carbon emission flow in networks. Sci Rep 2012;2(1):479.
[30] Li J, Ge S, Xu Z, Liu H, Li J, Wang C, et al. A network-secure peer-to-peer trading framework for electricity–carbon integrated market among local prosumers. Appl Energy 2023;335:120420.
[31] Zhang P, Mansouri SA, Jordehi AR, Tostado-Véliz M, Alharthi YZ, Safaraliev M. An ADMM-enabled robust optimization framework for self-healing scheduling of smart grids integrated with smart prosumers. Appl Energy 2024;363:123067.
[32] Xia Y, Xu Q, Huang Y, Liu Y, Li F. Preserving privacy in nested peer-to-peer energy trading in networked microgrids considering incomplete rationality. IEEE T Smart Grid 2022;14(1):606–22.
[33] Najafi A, Pourakbari-Kasmaei M, Jasinski M, Contreras J, Lehtonen M, Leonowicz Z. The role of EV based peer-to-peer transactive energy hubs in distribution network optimization. Appl Energy 2022;319:119267.
[34] Liu Y, Sun C, Paudel A, Gao Y, Li Y, Gooi HB, et al. Fully decentralized P2P energy trading in active distribution networks with voltage regulation. IEEE T Smart Grid 2022;14(2):1466–81.